PAPER

Influence of the capping layer material on the interfacial Dzyaloshinskii–Moriya interaction in Pt/Co/capping layer structures probed by Brillouin light scattering

IOP Publishing Journal of Physics D: Applied Physics
J. Phys. D: Appl. Phys. **52** (2019) 125002 (7pp) https://doi.org/10.1088/1361-6463/aafdf5

Influence of the capping layer material on the interfacial Dzyaloshinskii–Moriya interaction in Pt/Co/capping layer structures probed by Brillouin light scattering

M Belmeguenai[1,3], Y Roussigné[1], S M Chérif[1], A Stashkevich[1], T Petrisor Jr[2] and M Nasui[2] and M S Gabor[2,3]

[1] LSPM, CNRS-Université Paris 13, Sorbonne Paris Cité, 99 Avenue Jean-Baptiste Clément Université Paris 13, 93430 Villetaneuse, France
[2] Physics and Chemistry Department, Center for Superconductivity, Spintronics and Surface Science, Technical University of Cluj-Napoca, Str. Memorandumului, 400114 Cluj-Napoca, Romania

E-mail: belmeguenai.mohamed@univ-paris13.fr and mihai.gabor@phys.utcluj.ro

Received 19 October 2018, revised 4 January 2019
Accepted for publication 11 January 2019
Published 28 January 2019

Abstract

Co ultrathin films, of various thicknesses (0.8 nm $\leqslant t_{Co} \leqslant$ 2.5 nm), have been grown by sputtering on Si substrates, using Pt buffer layers and different capping layers (Cu, Ir, MgO and Pt). The x-ray diffraction revealed that our films have a (1 1 1) out-of-plane texture with various degrees of strains. Their magnetic properties have been studied by vibrating sample magnetometry (VSM) and Brillouin light scattering (BLS) in the Damon–Eshbach geometry. VSM characterizations revealed that films with Co thickness below (above) the spin reorientation transition thickness, which is capping layer dependent, are perpendicularly (in-plane) magnetized, suggesting the existence of an interface anisotropy. The surface anisotropy constant was found to be 1.42 $\pm$ 0.02 erg cm^{-2} and of 1.33 $\pm$ 0.02 erg cm^{-2} for the Pt/Co/Cu and Pt/Co/Ir samples, respectively, suggesting that it is due to the Pt/Co interface and that the top Co/Cu, Co/Pt or Co/Ir interfaces have a minor contribution. A lower value of 1.07 $\pm$ 0.02 erg cm^{-2} has been obtained for Pt/Co/MgO most probably due to over-oxidation of Co at the Co/MgO interface. The BLS measurements revealed a pronounced nonreciprocal spin waves propagation, due to the interfacial Dzyaloshinskii–Moriya interaction (iDMI) induced by Pt interface with Co, which increases with decreasing Co thickness. The magnetic dead layer has been taken into account to precisely determine the surface iDMI constant D_s estimated at -0.8 pJ m^{-1}, -1.05 pJ m^{-1} and -0.95 pJ m^{-1}, respectively for Pt/Co/Ir, Pt/Co/Cu and Pt/Co/MgO for sample thicknesses where a linear thickness dependence of the effective iDMI constant has been observed.

Keywords: Dzyaloshinskii–Moriya interaction, interface effects, Brillouin light scattering, spin waves, perpendicular magnetic anisotropy

(Some figures may appear in colour only in the online journal)

Introduction

The ultrathin character of magnetic heterostructures, especially those involving heavy metal films, leads to the emergence of several interesting interface effects [1–5], important for spintronic applications. In these systems, the so-called interfacial Dzyaloshinskii–Moriya exchange interaction (iDMI) [6, 7] is a consequence of the inversion symmetry breaking and of the presence of a heavy metal at interfaces. Unlike the Heisenberg exchange interaction (usually leading to collinear magnetic

[3] Authors to whom any correspondence should be addressed.

structures), the iDMI favors canted neighboring spins leading to various magnetization structures at the nanoscale, such as helices [8] and skyrmions [9–11] with a given chirality. Consequently, iDMI is currently under intensive research [12–14], due to its potential applications in the field of spintronics, aiming to quantify and to tune iDMI to engineer a desirable function.

The quantification of iDMI in different material systems consists of determining its effective (D_{eff}) or surface (D_s) constants [12] using reliable techniques. Today, it is well accepted that Brillouin light scattering (BLS) is the most direct and efficient method for iDMI characterization since few parameters are required for the experimental data fit. In fact, iDMI leads to a different energy (non-reciprocity) of two spin waves (SW) having the same wavelength and propagating along two opposite directions [9]. It is manifested by a difference between the frequencies of these two SWs. The DMI constant determination by BLS is thus reduced to this simple frequency difference measurement, making this technique simple, efficient, reliable and straightforward since it can simultaneously detect SWs propagating in the opposite directions.

Tuning the iDMI passes through knowing both iDMI constant sign and value for engineering the desired stacks presenting the suitable iDMI constant. Consequently, Pt-based heterostructures have been the most widely investigated due to their relatively high iDMI constant. Although the strong iDMI constant is usually obtained in Pt-based systems, the capping layer can influence the total value of the iDMI (and even cancel it especially if a heavy metal is used) since iDMI is sensitive to disorder, defects and atom arrangement at the interfaces. This offers the possibility of tuning the iDMI value by judicious choice of the different materials of the stack. Moreover, Boulle *et al* [15] suggested that the higher reported iDMI constant for Pt/Co/MgO systems can thus be explained by a significant additional contribution at the Co/MgO interface, which has the same sign as the one at the Pt/Co interface and thus enhances the total DMI. It is of great interest for applications and fundamental research to investigate the iDMI in Pt-based stacks, where different capping materials are used. Therefore, considering MgO, Ir and reference metal (Cu) could be helpful to identify the contributions of each interface.

In this paper, we address the thickness dependence of the iDMI in Pt/Co/*X*, where *X* is Pt, Cu, MgO and Ir. For this BLS technique, where the wave-vector of the SW is determined by the wavelength and the angle of incidence of the laser beam, combined with vibrating sample magnetometry (VSM) and x-ray diffraction (XRD) are used. We showed that the iDMI is mainly induced by Pt/Co interface and no significant contribution from MgO or Cu has been observed. The observed contribution of the Co/Ir interface will be discussed below.

Experimental techniques

All the samples studied here were grown at room temperature on thermally oxidized silicon substrates in a magnetron sputtering system having a base pressure lower than 2×10^{-8} Torr. The samples have the following structure: Si/SiO_2//Ta (3 nm)/Pt (3 nm)/Co (t_{Co})/*X*/Ta (3 nm), where *X* stands for Ir (3 nm), Cu (3 nm), Pt (3) or MgO (1 nm), depending on the sample. The metallic layers were grown by dc sputtering under an argon pressure of 1 mTorr, while the MgO layer was grown by rf sputtering under an argon pressure of 10 mTorr. The 3 nm thick Ta buffer layer was grown directly on the substrate to improve the roughness and to facilitate the (1 1 1) texturing of the upper Pt layer. An additional 3 nm thick Ta capping layer was deposited to protect the samples from oxidation due to air exposure. Although Ta is a heavy metal, the iDMI constant induced by Ta is very weak (less than 0.035 mJ/m^2 for Ta/CoFeB interface [13]). Moreover, since in the studied systems here Ta is not in direct contact with the Co, we expect that its contribution to the total iDMI is all the more reduced and can be neglected in our systems. Therefore, no iDMI contribution from Ta is expected. The static magnetic properties of samples have been investigated using VSM. The structure of samples has been characterized by XRD experiments using a four-circle diffractometer. BLS has been used, in the Damon–Eshbach configuration, to investigate the iDMI in all the samples. For this, an in-plane magnetic field (which is sample dependent), significantly high to saturate the magnetization in the film plane, has been applied and the BLS spectra (intensity versus the frequency) have been recorded after accumulation up to 12 h for each laser incidence angle (wave vector). The simultaneously detected Stokes (S) and anti-Stokes (aS) frequencies were determined from the Lorentzian fit to the BLS spectra.

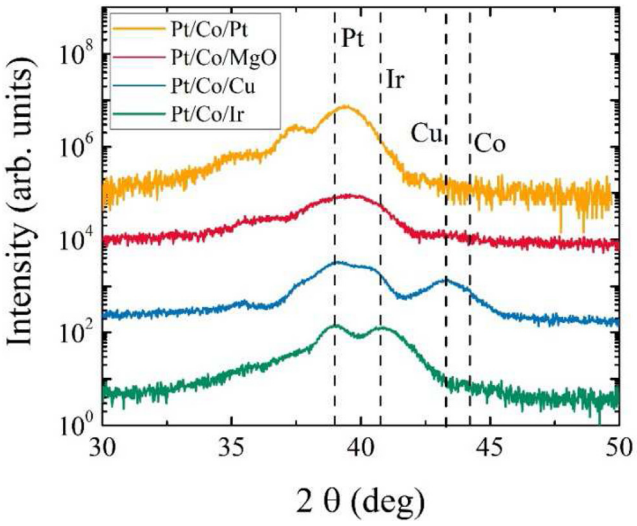

Figure 1. $2\theta/\omega$ XRD patterns measured for representative Pt/Co/MgO, Pt/Co/Ir and Pt/Co/Cu samples having nominal Co layer thickness of 1.6 nm and a Pt/Co/Pt sample with a nominal Co layer thickness of 1 nm. The vertical dashed lines indicate the position of the Pt (1 1 1) and Ir (1 1 1) reflections recorded for control samples, and the positions of the Cu (1 1 1) and Co (1 1 1) expected bulk reflections. The experimental data have been shifted vertically for clarity.

Results and discussions

Figure 1 shows $2\theta/\omega$ XRD patterns measured for representative Pt/Co/MgO, Pt/Co/Ir and Pt/Co/Cu samples having nominal Co layer thickness of 1.6 nm and a Pt/Co/Pt sample with

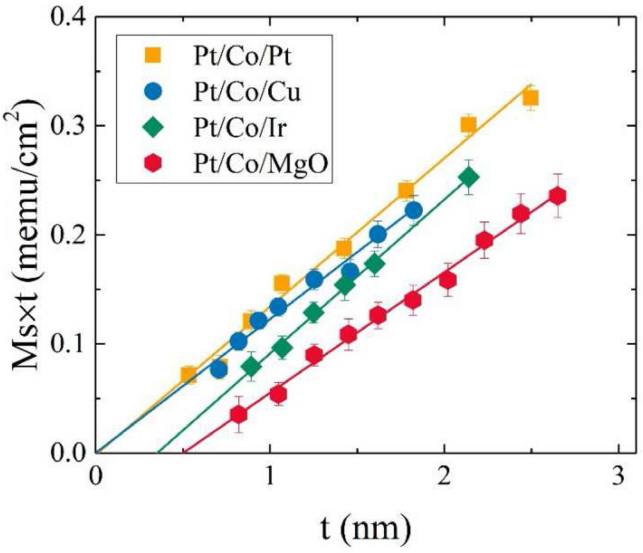

Figure 2. The surface magnetic moment ($M_s \times t$) versus the thickness of the Co layers for the four types of samples. Symbols refer to experimental data and lines are linear fits.

a nominal Co layer thickness of 1 nm. The data shown here were measured in a relatively narrow 2θ angle window around the expected positions of the (1 1 1) type reflections of Pt, Ir, Co and Cu. However, it should be mentioned that measurements on a wider 2θ range did not show the presence of other reflections except the (1 1 1) type, which indicates that our films have a (1 1 1) out-of-plane texture. In the case of the Pt/Co/Pt sample, the diffraction pattern shows a main peak at an angular position just above the Pt (1 1 1) reflection which was measured in a Si/SiO_2//Ta (3 nm)/Pt (3 nm)/Ta (3 nm) control sample. The shift to higher angles is owed to the strain in the system and it is due to the difference in the (1 1 1) lattice planes spacing of Pt ($d_{111} = 0.2265$ nm) and Co ($d_{111} = 0.2047$ nm). Asymmetric satellite peaks are also observable, with the most intense one being situated in the lower angles part, which is typical for a strained heterostructure [16]. In the case of the Pt/Co/MgO sample, the diffraction pattern shows a main peak close to the position of the Pt (1 1 1). Asymmetric satellite peaks can also be observed. In the case of the Pt/Co/Cu sample, the main maxima corresponding to the Pt (1 1 1) reflection is highly strain distorted. This is expected since, this type of sample is under the highest degree of strain due to the difference in the (1 1 1) lattice planes spacing of Pt ($d_{111} = 0.2265$ nm) and both Co ($d_{111} = 0.2047$ nm) and Cu ($d_{111} = 0.208$ nm). Regarding this sample, another peak is visible corresponding to the Cu (1 1 1) reflection. For the Pt/Co/Ir sample, the diffraction pattern consists of a broad peak with two local maxima corresponding to the Pt and Ir (1 1 1) reflections. For all the samples, no clear Co peak can be observed, most likely due to the low diffracted signal resulting from the relative low thickness of the Co layer in conjunction with its relatively low atomic scattering factor. These structural observations indicate that all types of samples have a (1 1 1) out-of-plane texture with a different degree of strain.

The magnetic properties of the Co films depend both on their thickness and on the nature of the top interface. Figure 2 shows the surface magnetic moment ($M_s \times t$) versus the nominal thickness of the Co layers for the four types of samples. Here, the slope of the linear fit of the data gives the mean saturation magnetization (M_s), while the horizontal axis intercept gives the extent of the magnetic dead layer (MDL). M_s shows a value of 1215 ± 55 emu cm^{-3} for the Pt/Co/Cu and a slightly smaller value of 1100 ± 50 emu cm^{-3} for the Pt/Co/MgO samples. The decrease of M_s for Pt/Co/MgO samples is most likely attributed to the oxidation of the upper Co layer interface in contact with MgO [17]. An increase of M_s to 1400 ± 70 emu cm^{-3} and 1380 ± 60 emu cm^{-3} can be observed in the case of Pt/Co/Ir and Pt/Co/Pt samples, respectively. This is most likely due to proximity induced magnetization at the Co/Ir and Co/Pt interfaces [18]. This corresponds to a change in film magnetization of 15% which is in good agreement with the reported values for Ir/Co[18]. No MDL was observed in the case of the Pt/Co/Cu, while an MDL of about $t_d = 0.36$ nm and 0.5 nm were determined for the Pt/Co/Ir and Pt/Co/MgO samples, respectively. The presence of an MDL, in the case of the Pt/Co/MgO samples, could be associated with a partial oxidation of Co when MgO is deposited on top. In the case of the Pt/Co/Ir, we attribute the MDL to the intermixing at the Co/Ir interface [19]. The absence of an MDL in the case of the Pt/Co/Cu sample is consistent with the lack of intermixing at the Co/Cu interface due to the immiscibility of the two materials [20].

Figure 3 shows representative hysteresis loops measured for two Pt/Co/Cu samples with the magnetic field applied perpendicular or parallel with the films surface. Two types of behaviors can be observed. Below the spin reorientation transition thickness (t_{SRT}), as in the case of the sample with the 1 nm thick Co film, the samples show a perpendicular magnetic anisotropy (PMA). This is indicated by the square shaped out-of-plane hysteresis loop (figure 3(b)) and by the in-plane hysteresis loop (figure 3(a)), which has a shape typical for a magnetization hard axis, showing a continuous rotation of the magnetization up to saturation. Above t_{SRT}, as in the case of the sample with the 1.8 nm thick Co film, the samples show in-plane magnetic anisotropy, the easy axis of the magnetization is rotated in-plane (figure 3(c)) and the hard axis of magnetization out-of-plane (figure 3(d)). It should be mentioned that the other types of samples show similar behaviors, with t_{SRT} depending on the nature of the Co overlayer.

To get more insight into the magnetic anisotropy of the structures, we have calculated the effective PMA constant using the relation: $K_{eff} = M_s H_s/2$, where H_s is the saturation field determined from the hard axis hysteresis loops. It should be mentioned that H_s was taken to be negative (positive) when Co layer was in-plane (out-of-plane) magnetized. The effective magnetic anisotropy can be separated into a volume and a surface contribution using the phenomenological relation [21]: $K_{eff} \times t_{eff} = K_v \times t_{eff} + K_s$; with K_v the volume (including magnetocrystalline, shape and strain related anisotropies) and K_s the surface components, respectively. The effective thickness (t_{eff}) of the Co layers was obtained by subtracting the thickness of the MDL from the nominal one. Figure 4 shows the effective anisotropy times the effective thickness $K_{eff} \times t_{eff}$ versus the effective thickness of the Co layers. A pronounced deviation from the linear behavior

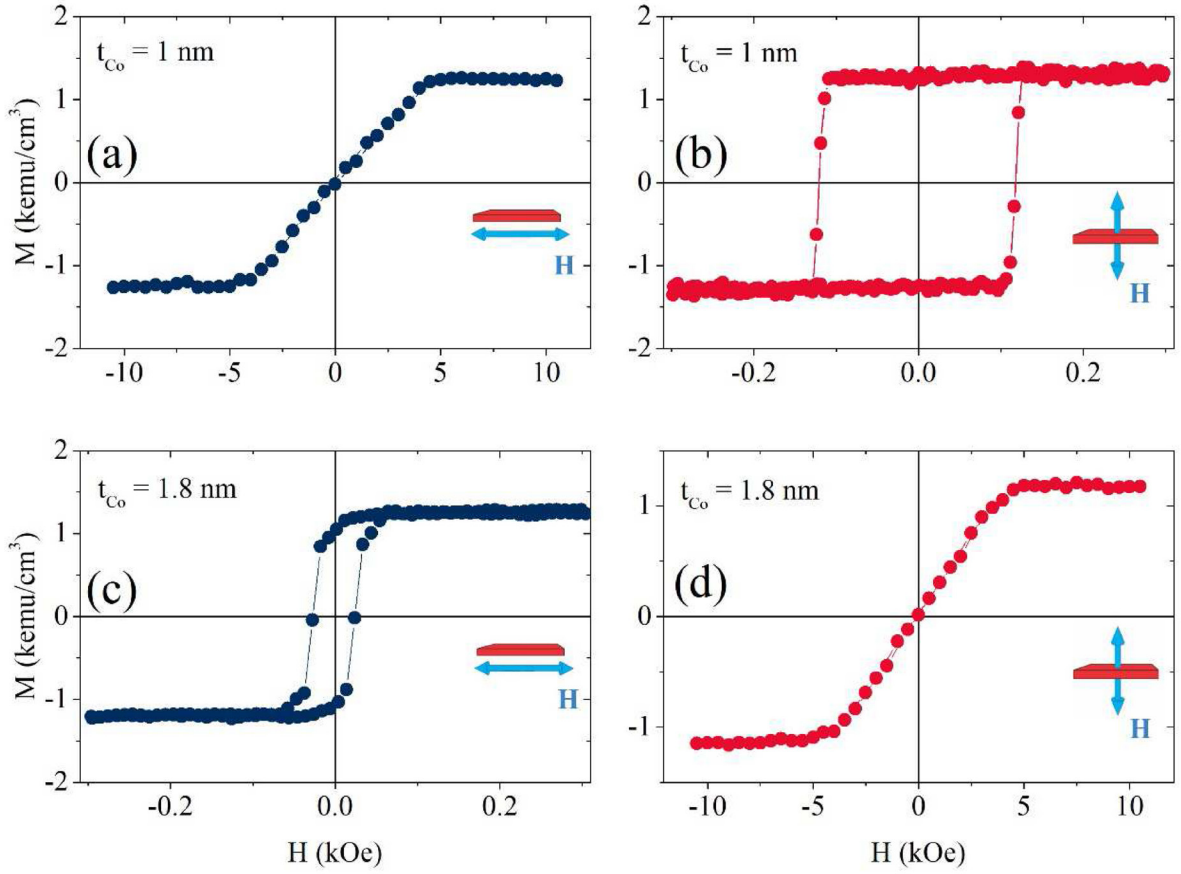

Figure 3. In-plane ((a) and (c)) and out-of-plane ((b) and (d)) hysteresis loops measured for two Pt/Co/Cu samples with a Co layer thickness of 1 nm and 1.8 nm, respectively.

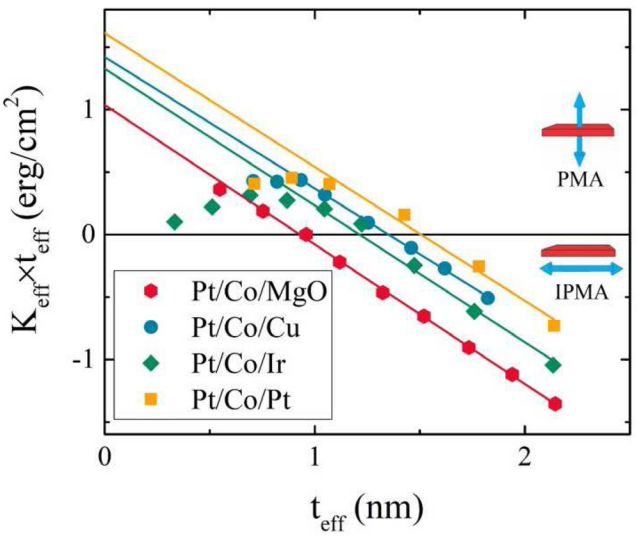

Figure 4. The effective anisotropy times the effective thickness $K_{eff} \times t_{eff}$ versus the effective thickness of the Co layers. Symbols are experimental data while lines are results of linear fits. The sketch refers to Co thicknesses where samples present a perpendicular magnetic anisotropy (PMA) and an in-plane magnetic anisotropy (IMA).

for the thinner Co films is observed for Pt/Co/Ir, suggesting the existence of two regimes. This deviation from the linear behavior is frequently reported for magnetic thin films and could be most likely attributed to interface degradation for thinner Co films, to coherent and incoherent growth of Co induced by the strain misfit of Co and buffer or capping layers, to the intermixing at the top Co interface and to the decrease of the Curie temperature for the ultrathin Co films [20]. K_v and K_s were extracted using the phenomenological relation by performing linear fits of data in the linear regime. K_s shows rather similar values of 1.42 ± 0.02 erg cm^{-2} and of 1.33 ± 0.02 erg cm^{-2} for the Pt/Co/Cu and Pt/Co/Ir samples, respectively. In the case of the Pt/Co/Pt samples, K_s is around 1.61 ± 0.08 erg cm^{-2}. This seems to indicate that K_s is mainly due to the Pt/Co interface and that the top Co/Cu, Co/Pt or Co/Ir interfaces have a minor contribution to K_s. For these samples, K_v is practically equal to the shape anisotropy ($2\pi M_s^2$), the magneto-crystalline anisotropy being negligible suggests that our Co films have a fcc crystal structure [22]. In the case of the Pt/Co/MgO samples, K_s has a lower value of 1.07 ± 0.02 erg cm^{-2}, while K_v deviates from the shape anisotropy with non-negligible amount of: $K_v - 2\pi M_s^2 = (3.7 \pm 0.9)$ Merg cm^{-3}. While the decrease of K_s might be due to over-oxidation of Co alt the Co/MgO interface [17, 23], the origins of K_v remains unclear.

BLS was used to investigate the iDMI in all the samples. The typical spectra recorded for some representative heterostructures are shown in figure 5 for $k_{sw} = 20.45$ μm^{-1}. Note the lower signal to noise ratio for Pt/Co/Ir, despite roughly the same accumulation time with the other systems, suggesting the lesser quality of this heterostructure. This is

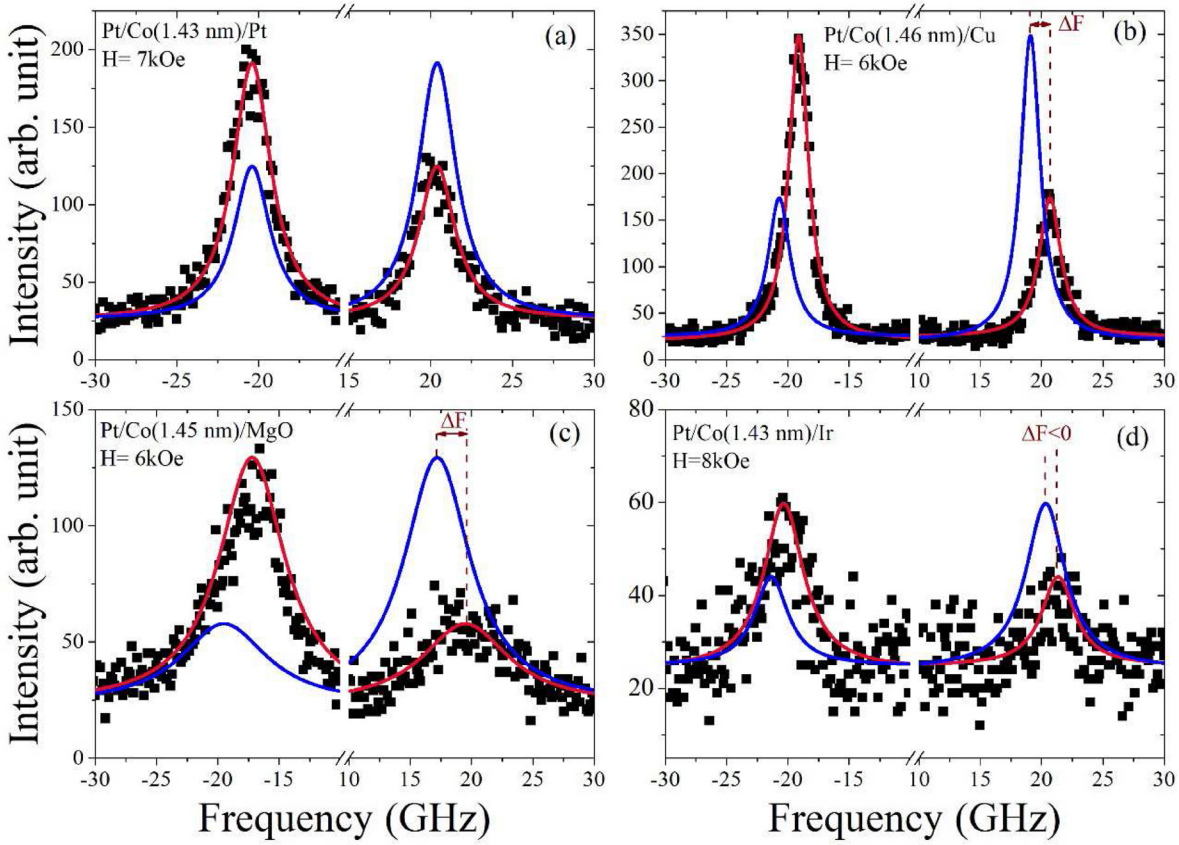

Figure 5. BLS spectra measured for (a) Pt/Co (1.43 nm)/Pt, (b) Pt/Co (1.46 nm)/Cu, (c) Pt/Co (1.435)/MgO and (d) Pt/Co (1.43 nm)/Ir systems, at various in-plane applied magnetic field values and at a characteristic SW-vector $k_{sw} = 20.45\ \mu m^{-1}$. Symbols refer to experimental data, and solid lines are the Lorentzian fits. Fits corresponding to negative applied fields (blue lines) are presented for clarity and direct comparison of the S and aS frequencies.

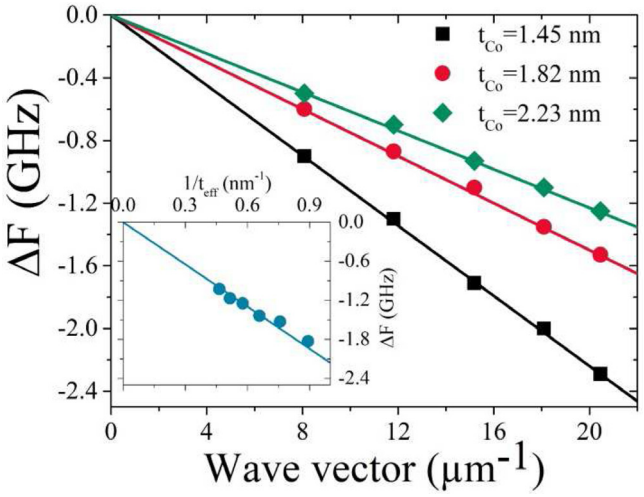

Figure 6. Wave vector (k_{sw}) dependence of the experimental frequency difference ΔF (symbols) for Pt/Co/MgO samples. Solid lines refer to linear fit using equation (1) and magnetic parameters given in the main text. The inset of the figure shows the thickness dependence of the frequency difference ΔF corresponding to $k_{sw} = 20.45\ \mu m^{-1}$. Symbols refer to experimental data, and straight solid lines are used for eye guides.

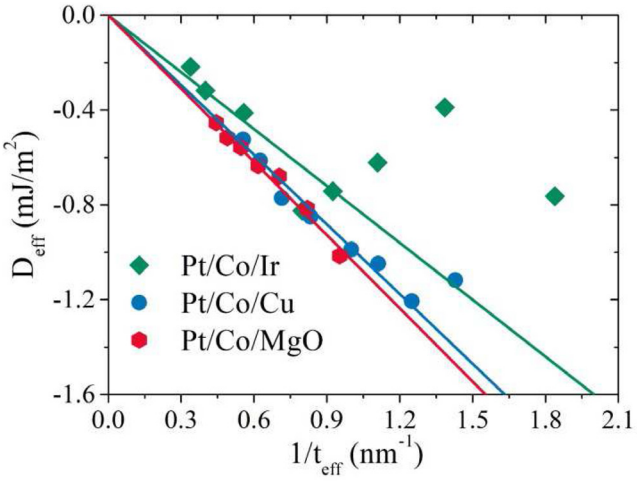

Figure 7. Thickness dependence of the effective iDMI constants extracted from fits of wave vector dependence of the frequency mismatch of the different studied systems. Solid lines refer to the linear fit.

consistent with the relative thick MDL determined from static magnetic measurements, attributed to the Co/Ir inter-diffusion. The spectra reveal the existence of both Stokes and anti-Stokes spectral lines and their frequencies are sample dependent due to the presence of PMA. For a symmetrical Pt/Co/Pt control sample (figure 5(a)), despite of the use of a heavy metal (Pt) in contact with the Co, the Stokes and anti-Stokes frequency (F_S and F_{aS}, respectively) lines are the same due to the absence of any interface symmetry breaking. However, the use of a different material as a capping layer

Table 1. Magnetic parameters obtained from the best fits of BLS and VSM results with the model described in the main text. Within the measurement precision, our iDMI constants for Pt/Co/Pt are zero.

System	$\gamma/2\pi$ (GHz T^{-1})	M_s (emu cm^{-3})	t_d (nm)	D_s (pJ m^{-1})	K_s (mJ m^{-2})
Pt/Co/Ir	30.35	1400 ± 70	0.38 ± 0.027	-0.8 ± 0.07	1.33 ± 0.02
Pt/Co/Cu	30.35	1215 ± 55	0	-1.05 ± 0.08	1.42 ± 0.02
Pt/Co/MgO	30.35	1100 ± 50	0.5 ± 0.1	-0.95 ± 0.06	1.07 ± 0.02
Pt/Co/Pt	30.35	1380 ± 60	0		1.61 ± 0.08

lifts the frequency degeneracy and leads to a SW non-reciprocity, resulting in a frequency difference between S and aS lines ($\Delta F = F_S - F_{aS}$). The variation of this frequency shifts (ΔF) versus k_{sw} is shown in figure 6 for Pt/Co/MgO system of different Co thicknesses, where a linear behavior can be observed. Note the negative sign of ΔF suggesting that the Pt buffer layer induces a negative iDMI effective constant. Since the inverse proportionality on the ferromagnetic layer thickness is usually a signature of an interface effect, the behavior of ΔF versus the effective thickness of Co (considering the MDL) in Pt/Co/MgO systems is shown in the inset of figure 6, for $k_{sw} = 20.45$ μm^{-1}. It can be observed that ΔF increases with the reciprocal effective thickness ($1/t_{eff}$) and approaches zero when t_{eff} tends to infinity, confirming the interfacial origin of the DMI. Since the iDMI is usually characterized by its effective (D_{eff}) or surface (D_s) constants [24], the experimental data shown on figure 6 have been fitted by the equation:

$$\Delta F = F_S - F_{aS} = \frac{2\gamma}{\pi M_S} D_{eff} k_{sw} = \frac{2\gamma}{\pi M_S} \frac{D_S}{t_{eff}} k_{sw}, \qquad (1)$$

where M_s is the magnetization at saturation, $\gamma/(2\pi) = 30.35$ GHz T^{-1} is the gyromagnetic ratio of Co and t_{eff} is the effective thickness of the Co layers. From slopes of k_{sw} dependences of ΔF shown in figure 6, the effective iDMI constants (D_{eff}) have been extracted for all systems. The evolution of the obtained values of D_{eff} as a function of the inverse of the Co films effective thickness ($1/t_{eff}$) are shown in figure 7, where a linear behavior can be observed for relatively thick films, as predicted theoretically. Note again the deviation from the linearity, as the effective thickness of Co approaches 1 nm. The linearity deviation is more pronounced for the Pt/Co/Ir confirming the lesser quality of this system, due to the Co/Ir interdiffusion, as mentioned above. The slower dependence of the D_{eff} for thinner Co layers is also most probably due to the degradation of the interface quality of the thin ferromagnetic layer, strain misfit of Co and capping layer or to the decrease in the Curie temperature. It is worth mentioning that for Pt/Co/Pt systems no significant frequency shift between S and aS lines have been measured at the maximal SW number (20.45 μm^{-1}) due to its stack symmetry. Therefore, we were not able to determine precisely the effective DMI constant. We thus just limited our investigation to check this stack symmetric for all Co thicknesses by measuring the frequency shift (at 20.45 μm^{-1}). Within the measurement precision, our iDMI constants for Pt/Co/Pt are zero. By the linear fit of the data in figure 7, for Co thickness range where the theoretical linearity of D_{eff} is observed, D_s has been determined and its values are summarized in table 1. Note the negative sign of iDMI in Pt/Co/X systems suggesting that this iDMI is mainly induced by Pt in such system. The lower value of the iDMI surface constant in Pt/Co/Ir with respect to Pt/Co/Cu and Pt/Co/MgO can be attributed to the reduction of the iDMI by the contribution of the Co/Ir since Pt/Co and Co/Ir interfaces have an opposite iDMI sign. However, the observed lower signal to noise ratio and the pronounced deviation from the linearity suggests that the lower iDMI is most probably due to the lesser quality of Pt/Co/Ir system. The mostly similar obtained values (in absolute values) for Pt/Co/Cu and Pt/Co/MgO is in good agreement with Ma *et al* [13], who reported the absence of iDMI in CoFeB/MgO. Moreover, the vanishing of the frequency difference (iDMI constant) that occurs for a symmetric Pt/Co/Pt structure confirms that the upper and bottom Co/Pt interfaces are similar. It is worth mentioning that iDMI is sample deposition condition dependent [14] and it is not surprising to have a discrepancy in the measured values between groups for the same system.

Finally, it worth mentioning that since both iDMI and interface anisotropy are related to spin orbit interaction at the interface and are sensitive to disorder, defects and atom arrangement at the interfaces, one can expect a correlation between these quantities. As we mentioned above, the observed similar deviation from the linearity for iDMI and effective anisotropy for thinner Co layers (see figures 4 and 7), most probably due to interface degradation and intermixing, suggests a possible correlation between PMA and iDMI due to the interfacial origin of both iDMI and PMA. However, since interface PMA results from the contribution of the two interfaces with the ferromagnetic layer while iDMI effect is due mostly to the interface with the heavy metal, it is not obvious to speculate about the correlation between iDMI and interface PMA. Furthermore in previous work [25], we reported that both iDMI and interface PMA of Pt/Co_2FeAl/MgO showed opposite trends with the annealing temperature: while the interface anisotropy increases, the iDMI surface constant decreases with increasing annealing temperatures. This again makes it difficult to speculate about the correlation between PMA and iDMI.

Conclusions

We have investigated the influence of capping layer in Pt/Co/X multilayers with X = Cu, Ir, MgO, Pt on iDMI and on interface perpendicular anisotropy. For each capping layer, a series of samples with various Co thicknesses has been studied. The VSM provided the surface and the volume anisotropy constant

values for each kind of capping layer while the SW frequency measurements allowed the determination of the iDMI magnitude. For the thicker samples ($1\,\text{nm} < t_{Co} < 2.5\,\text{nm}$), a linear reciprocal thickness dependence (following the theoretical model stipulating that $D_{eff} = D_s/t_{eff}$) of D_{eff} is observed allowing to determine D_s. For thinner samples, where a significant change of interfaces may occur, a deviation from the linear behavior (theoretical model) is revealed and D_s cannot be determined. The effective iDMI constant may drastically be reduced if the capping layer is not appropriate, especially for Ir capping layer. We conclude that while the capping layer in Pt/Co/Cu and Pt/Co/MgO systems has no measurable influence on the iDMI magnitude within the investigated Co thickness range because Co/*X* interface contribution to iDMI is likely much smaller than that of Pt/Co interface, the iDMI magnitude of Pt/Co/Ir has been decreased. When the top layer is made of Pt, its contribution to iDMI interaction completely cancels that of the bottom interface Pt/Co. This cancelation only occurs if the two Pt layers are similar, thus proving that in our samples the upper Pt layer has the same characteristics as the lower one.

Acknowledgments

This work has been supported by the Conseil regional d'Île-de-France through the DIM NanoK (BIDUL project). T P, M N and M S G acknowledge the financial support of the CNCS/UEFISCDI through PN-III-P1-1.1-TE-2016-2131-SOTMEM Grant No. 24/02.05.2018.

ORCID iDs

M Belmeguenai https://orcid.org/0000-0002-2395-1146
S M Chérif https://orcid.org/0000-0003-4350-9379
M S Gabor https://orcid.org/0000-0003-0888-0762

References

[1] Zhang S 2000 *Phys. Rev. Lett.* **85** 393
[2] Valenzuela S O and Tinkham M 2006 *Nature* **442** 176
[3] Werake L K, Ruzicka B A and Zhao H 2011 *Phys. Rev. Lett.* **106** 107205
[4] Costache M V, Sladkov M, Watts S M, van der Wal C H and van Wees B J 2006 *Phys. Rev. Lett.* **97** 216603
[5] Woo S, Mann M, Tan A J, Caretta L and Beach G S D 2014 *Appl. Phys. Lett.* **105** 212404
[6] Dzialoshinskii I E 1957 *J. Exp. Theor. Phys.* **5** 1259
[7] Moriya T 1960 *Phys. Rev.* **120** 91
[8] Kishine J and Ovchinnikov A S 2015 *Solid State Phys.* **66** 1–130
[9] Rößler U K, Bogdanov A N and Pfleiderer C 2006 *Nature* **442** 797
[10] Felser C 2013 *Angew. Chem., Int. Ed. Engl.* **52** 1631
[11] Nagaosa N and Tokura Y 2013 *Nat. Nanotechnol.* **8** 899
[12] Belmeguenai M, Adam J-P, Roussigné Y, Eimer S, Devolder T, Kim J-V, Cherif S M, Stashkevich A and Thiaville A 2015 *Phys. Rev.* B **91** 180405
[13] Ma X, Yu G, Tang C, Li X, He C, Shi J, Wang K L and Li X 2018 *Phys. Rev. Lett.* **120** 157204
[14] Wells A W J, Shepley P M, Marrows C H and Moore T A 2017 *Phys. Rev.* B **95** 054428
[15] Boulle O *et al* 2016 *Nat. Nanotechnol.* **11** 449
[16] Segmuller A and Blakeslee A E 1973 *J. Appl. Crystallogr.* **6** 19
[17] Yang Y, Yuan J, Qi L, Wang Y, Xu Y, Wang X, Feng Y, Xu B, Shen L and Wu Y 2017 *Phys. Rev.* B **95** 094417
[18] Ryu K-S, Yang S-H, Thomas L and Parkin S S P 2014 *Nat. Commun.* **5** 3910
[19] Gabor M S, Petrisor T Jr, Mos R B, Nasui M, Tiusan C and Petrisor T 2017 *J. Phys. D: Appl. Phys.* **50** 465004
[20] Bandiera S, Sousa R C, Rodmacq B and Dieny B 2011 *IEEE Magn. Lett.* **2** 3000504
[21] den Broeder F J A, Hoving W and Bloemen P J H 1991 *J. Magn. Magn. Mater.* **93** 562
[22] Suzuki T, Weller D, Chang C A, Savoy R, Huang T, Gurney B A and Speriosu V 1994 *Appl. Phys. Lett.* **64** 2736
[23] Dieny B and Chshiev M 2017 *Rev. Mod. Phys.* **89** 025008
[24] Belmeguenai M, Gabor M S, Roussigné Y, Stashkevich A, Chérif S M, Zighem F and Tiusan C 2016 *Phys. Rev.* B **93** 174407
[25] Belmeguenai M *et al* 2018 *Phys. Rev. Appl.* **9** 044044